

In-situ monitoring of fatigue of metastable austenitic steels with electromagnetic acoustic transducers, EMATs

Andreas Sorich^{*}, Marek Smaga, Dietmar Eifler

Institute of Materials Science and Engineering,
University of Kaiserslautern, P.O. Box 3049, D-67653 Kaiserslautern, Germany

*Corresponding author: sorich@mv.uni-kl.de

Abstract In this research work an in-situ method for the characterization of fatigue processes in metastable austenitic steels with electromagnetic acoustic transducers (EMATs) was developed. The austenitic steel AISI 347 (1.4550, X6CrNiNb1810) was investigated in isothermal total strain-controlled tests in the LCF-range at ambient temperature and 300 °C. By means of cross effects between physically based mechanical- and EMAT-measurements, a detailed characterization of cyclic hardening and softening processes as well as fatigue induced phase transformations and changes of specimens topography and crack initiation were performed.

Keywords Austenitic stainless steel, fatigue, phase transformation, α' -martensite, NDT, EMAT

1. Introduction

In power plants as well as in chemical plants, metastable austenitic steels are subjected to monotonic and cyclic thermo-mechanical loading [1-2]. The cyclic deformation behavior of metastable austenitic steels at ambient temperature (AT) and elevated temperature strongly depends on the deformation induced α' -martensite formation. This phase transformation from paramagnetic austenite (fcc) into ferromagnetic α' -martensite (bcc) leads to cyclic hardening and thus to an increase of the fatigue strength [2-4, 8]. At elevated temperatures no α' -martensite formation was observed in the LCF-range. Therefore the fatigue behavior at elevated temperatures depends basically on cyclic hardening processes due to an increase of dislocation density, followed by cyclic saturation and/or softening processes due to changes in dislocation arrangement and density and finally the formation and propagation of fatigue cracks [5-8]. The investigations are focused on the characterization of the fatigue processes at AT and 300 °C and the development of in-situ monitoring methods on the basis of electromagnetic acoustic measurements. EMATs, which generate ultrasonic waves directly in electrically conductive materials without the use of a couplant, were developed at the Fraunhofer Institute for Non-Destructive Testing (IZFP) Saarbrücken in Germany and calibrated to defined fatigue states in collaboration with the Institute of Materials Science and Engineering (WKK) at the University of Kaiserslautern in Germany [8]. The activities at WKK are focused on the characterization of the materials science aspects of the fatigue processes, while IZFP develops electromagnetic acoustic transducers.

2. Experimental procedures

2.1. Experimental setup

The fatigue tests were performed at different constant total strain amplitudes ($\epsilon_{a,t} = 0.8, 1.0, \text{ and } 1.2 \%$) at ambient temperature and 300 °C on a servo-hydraulic testing system with a strain ratio of $R_\epsilon = -1$ using triangular load-time functions and a frequency of 0.01 Hz. Figure 1 shows schematically the experimental setup for both temperatures. Besides electromagnetic non-destructive testing methods using EMAT and a Feritescope[®] sensor, full mechanical strain-stress hysteresis measurements were performed to allow a microstructure-related description of the cyclic deformation behavior of the metastable austenite. Electromagnetic acoustic transducers use electromagnetic fields to excite ultrasonic waves and therefore have the great advantage that

they can be used for ultrasonic measurements without a coupling medium between the transmitter/receiver and the test object. This set-up allows measurements on sensitive surfaces and objects also at elevated temperatures. Another advantage of EMATs is their very efficient generation of shear waves with both vertical and horizontal polarization for oblique angles of incidence as well as the generation of linearly, radially and elliptically polarized shear waves for the normal incidence [9].

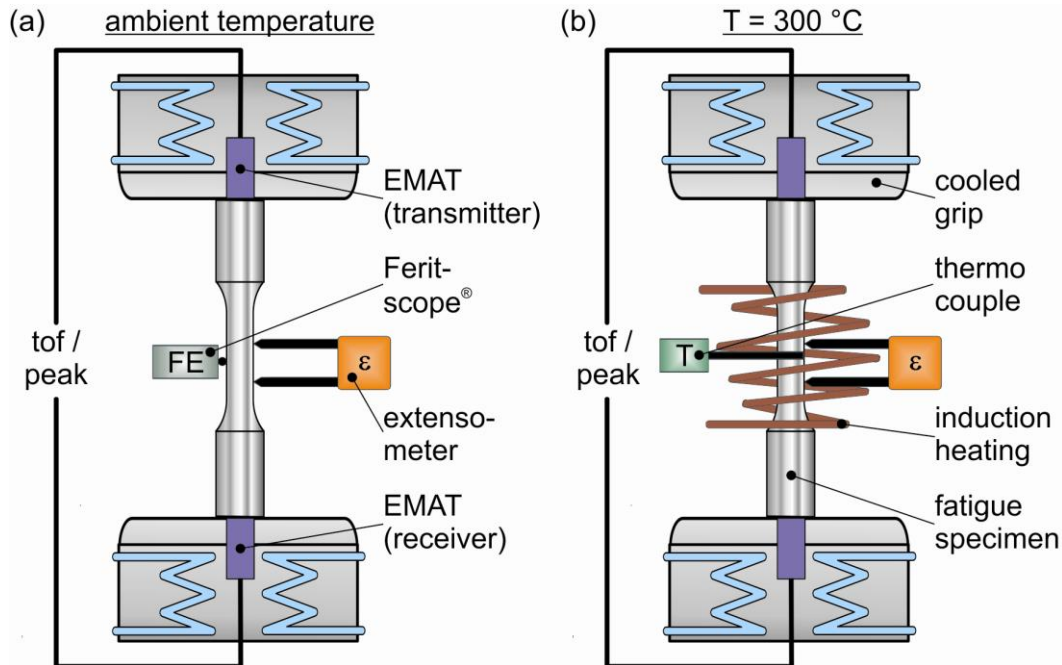


Figure 1. Schematic drawing of the experimental setup: ambient temperature (a) and $T = 300\text{ }^{\circ}\text{C}$ (b)

EMATs generate ultrasonic waves by means of Lorentz forces, magnetostriction or by magnetic forces. Ultrasound generation by means of magnetostriction or magnetic forces requires ferromagnetic materials. Thus, since the investigated material in this project is a paramagnetic austenitic steel, the ultrasonic waves are generated only by Lorentz forces. The excitation of ultrasound by EMATs is performed by the superposition of high frequency eddy currents, induced by a coil with a geometry matched to the wave pattern, and a static or low-frequency magnetic field (Figure 2). The waves are picked up by a receiving coil geometrically identical to the transmitter coil. In this project radially polarized shear waves are generated by the transmitter at the one end and the receiver at the other end [9].

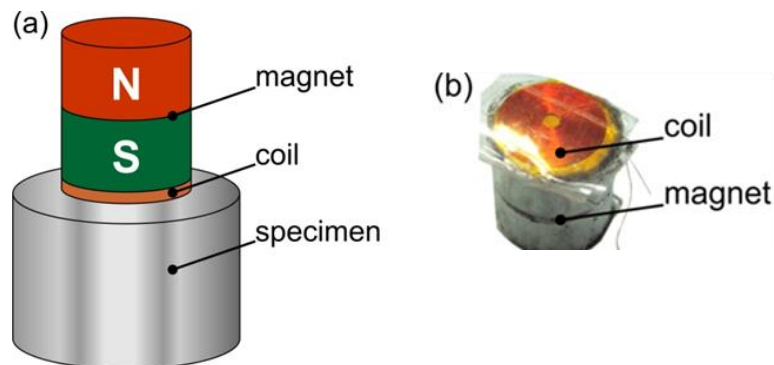


Figure 2. Assembling of an electromagnetic acoustic transducer for radially polarized shear waves: schematic picture (a), photo of a probe (b)

2.2. Material

The investigated material was the Nb-stabilized metastable austenitic stainless steel AISI 347 (1.4550, X6CrNiNb1810). The chemical composition is given in Table 1. The calculation of the austenite stability parameters (e.g. $M_{d30} = 26$ °C by Angel) results in a metastable state of the test material at ambient temperature. This calculation gives an approximate value, which means, that at a sufficient plastic deformation at ambient temperature an austenite-martensite-transformation can be expected. The initial microstructure (Figure 3) of the investigated steel has a mean grain size of 120 μm and a HV10 hardness of 140 HV. Also Nb-carbides were observed. The chemical composition of these carbides was analyzed via EDX-mapping. As expected the tensile strength, ultimate strain and reduction in area decrease with increasing temperature. At ambient temperature, at a plastic deformation of 66 %, 4.41 FE-% α' -martensite was formed. The α' -martensite formation starts at a total strain of 22 %. Magnetic measurements and micrographs after tensile tests at 300 °C indicated no α' -martensite formation.

Table 1. Chemical composition in weight-%

C	Cr	Ni	Nb	N	Si	Mn	P	S	Al
0.040	17.600	10.640	0.620	0.007	0.410	1.830	0.020	0.007	0.016
Ti	Sn	Mo	W	Cu	Co	V	Pb	B	Fe
0.020	0.008	0.290	0.030	0.060	0.010	0.070	< 0.008	< 0.005	bal.

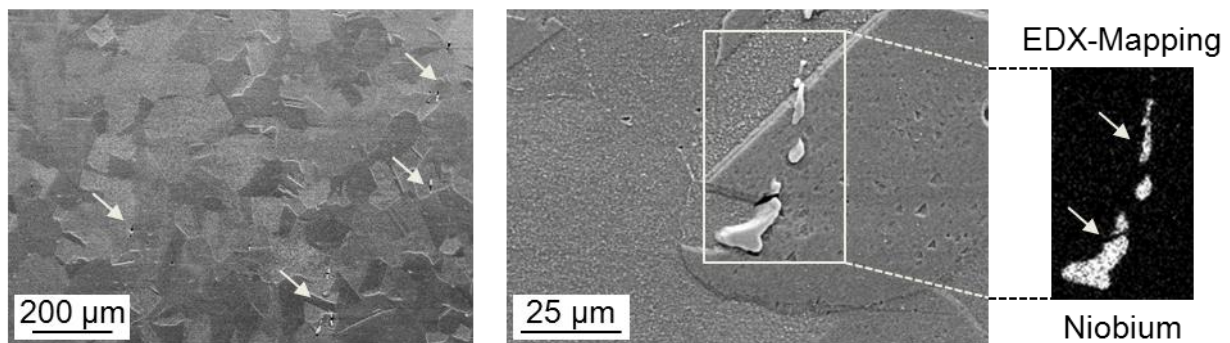


Figure 3. SEM-micrograph and EDX-analyses of AISI 347 in solution annealed state

3. Results and discussion

3.1. Evaluation of the fatigue behavior with deformation induced α' -martensite formation

Figure 4 shows the development of the stress amplitude σ_a and ferromagnetic martensite fraction ξ (Figure 4a), the change in the mean value of time of flight $\Delta\text{tof}_{\text{mean}}$ (Figure 4b) and the change in the mean value of the electromagnetically activated ultrasonic amplitude $\Delta\text{peak}_{\text{mean}}$ (Figure 4c) versus the number of cycles N in fatigue tests at ambient temperature.

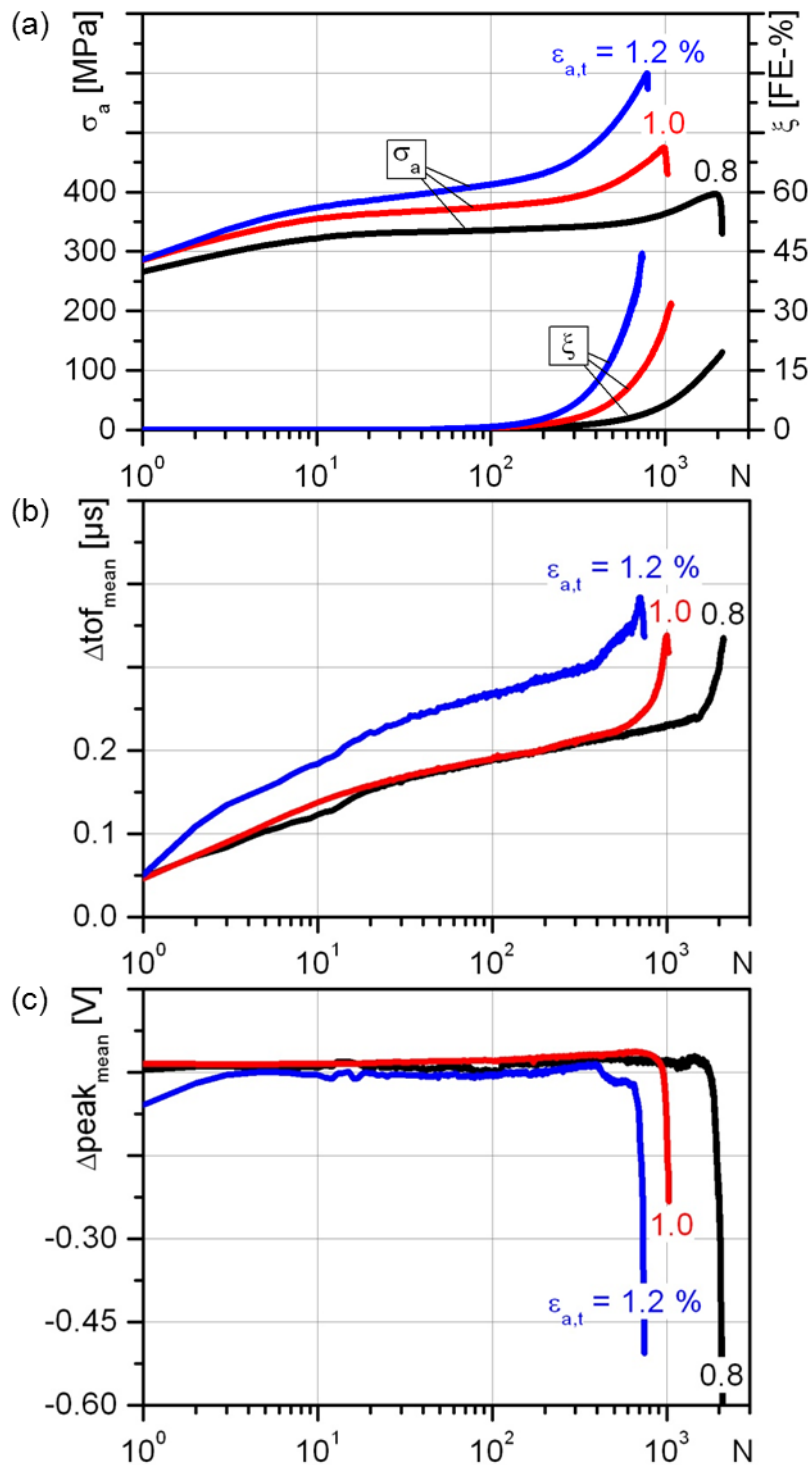


Figure 4. Stress amplitude σ_a and ferromagnetic martensite fraction ξ (a), change in $\Delta \text{tof}_{\text{mean}}$ (b) and change in $\Delta \text{peak}_{\text{mean}}$ (c) vs. number of cycles N at ambient temperature

Due to the change of tof and peak within one cycle, caused by the elongation of the specimen and change of the stress state of the specimen (Figure 7), an arithmetic mean value per load cycle for tof and peak was chosen to characterize the fatigue behavior [8]. The cyclic deformation behavior of the investigated austenite at ambient temperature is predominantly determined by the deformation induced austenite-martensite transformation. After a load dependent number of cycles N , the formation of α' -martensite starts and increases continuously with increasing number of cycles until specimen failure (Figure 4a). The σ_a , N -curves illustrate the cyclic hardening processes, which lead

for $\varepsilon_{a,t} = 1.2\%$ to a maximum stress amplitude in the range of the tensile strength $\sigma_f = 569$ MPa of the solution-annealed austenite. Due to an increase of the dislocation density, formation of deformation-induced α' -martensite, development of intrusion and extrusions at the specimen surface and finally the formation of micro- and macro-cracks a continuous increase of the change in the mean value of time of flight Δt_{of_mean} from the beginning of the fatigue loading up to specimen failure was observed at ambient temperature (Figure 5). However the electromagnetically activated ultrasonic amplitude $\Delta peak_{mean}$ shows no significant changes until the formation and propagation of micro- and macro-cracks (comp. Figure 4c with Figure 5). Because Δt_{of_mean} is more sensitive to microstructural fatigue effects, which lead to an increase of Δt_{of_mean} until specimen failure, it isn't possible to detect the state of macro-crack formation and propagation. The change in the mean value of the ultrasonic amplitude $\Delta peak_{mean}$ shows in contrast to Δt_{of_mean} a decrease at the fatigue state of macro-crack formation and propagation. Thus it is possible to detect specimen failure at an earlier fatigue state.

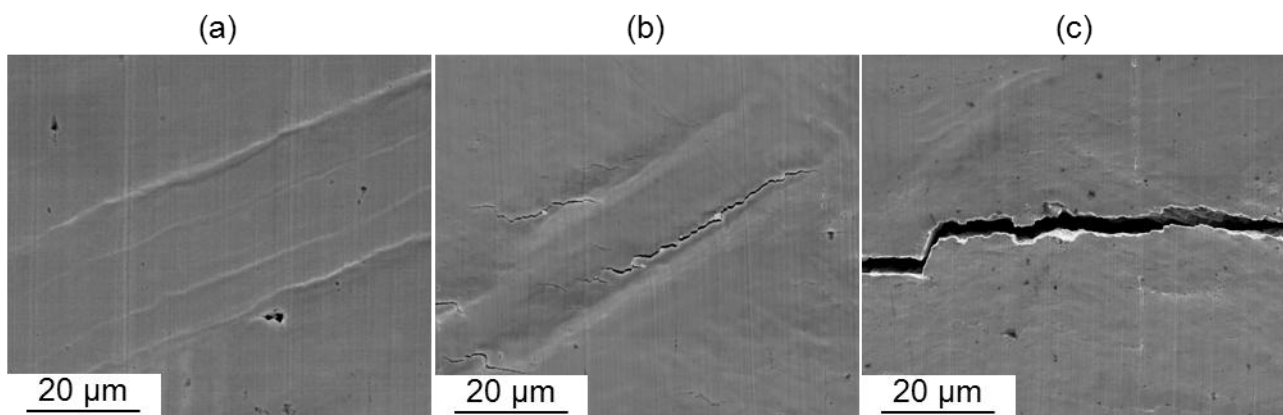


Figure 5. Changes in specimen surface topography at defined fatigue states at ambient temperature: N = 100 slip bands (a), N = 400 micro-cracks (b) and N = 900 macro-crack (c)

3.2. Evaluation of the fatigue behavior without deformation induced α' -martensite formation

Figure 6 shows the development of the stress amplitude σ_a (Figure 6a), the change in the mean value of time of flight Δt_{of_mean} (Figure 6b) and the change in the mean value of the electromagnetically activated ultrasonic amplitude $\Delta peak_{mean}$ (Figure 6c) versus the number of cycles N for fatigue tests at 300 °C. The cyclic deformation behavior of the investigated metastable austenite at this temperature is characterized by initial cyclic hardening, followed by cyclic softening before the final stress amplitude drop, associated with the propagation of a fatigue crack. At 300 °C no martensite formation occurs and compared to ambient temperature the stress amplitude is significantly lower. In the Δt_{of_mean} , N-curves generally three sections over the fatigue life were observed. In the first section Δt_{of_mean} shows similar to σ_a and tests at ambient temperature an initial increase caused by dislocation hardening. The second section follows with a decrease of Δt_{of_mean} due to cyclic softening. The third one shows a secondary increase of Δt_{of_mean} , which is mainly affected by the development of intrusions and extrusions at the specimen surface and finally the initiation and propagation of fatigue cracks (Figure 6b). In analogy to the investigations at ambient temperature, the change in the mean value of the ultrasonic amplitude $\Delta peak_{mean}$ shows in contrast to Δt_{of_mean} a decrease at the fatigue state of macro-crack formation and propagation.

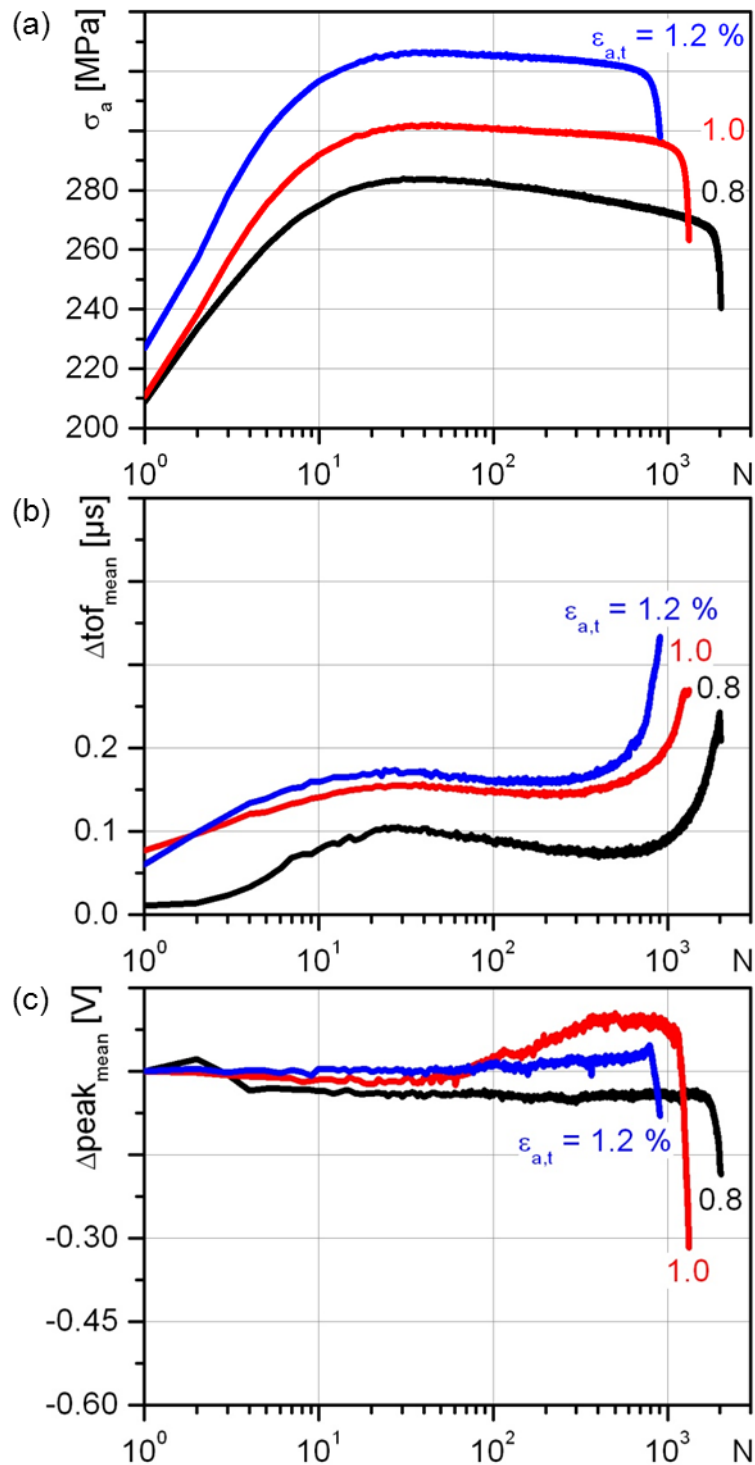


Figure 6. Stress amplitude σ_a (a), change in Δtof_{mean} (b) and change in $\Delta peak_{mean}$ (c) vs. number of cycles N at $T = 300 \text{ }^\circ\text{C}$

3.3. In-situ monitoring of fatigue damage by means of cross effects between mechanical and EMAT data

Besides the conventional characterization of the cyclic deformation behavior using stress-strain-hysteresis measurements, far-reaching cross effects of physically based data from electromagnetically activated ultrasonic measurements and mechanical strain measurements can be used for in-situ monitoring of fatigue processes. Figure 7 shows stress-strain-hysteresis at defined

number of cycles (N) during total-strain-controlled LCF-fatigue tests with $\varepsilon_{a,t} = 1\%$ at ambient temperature (Figure 7a) and at 300 °C (Figure 7b). The development of stress amplitude and/or plastic strain amplitude is used usually for the characterization of cyclic softening or hardening processes (comp. Figure 4a and 6a). The change of the shape (A) of σ - ε -hysteresis loop occurs due to macro-crack formation at $N = 1020$ at ambient temperature and at $N = 1300$ in the test at 300 °C.

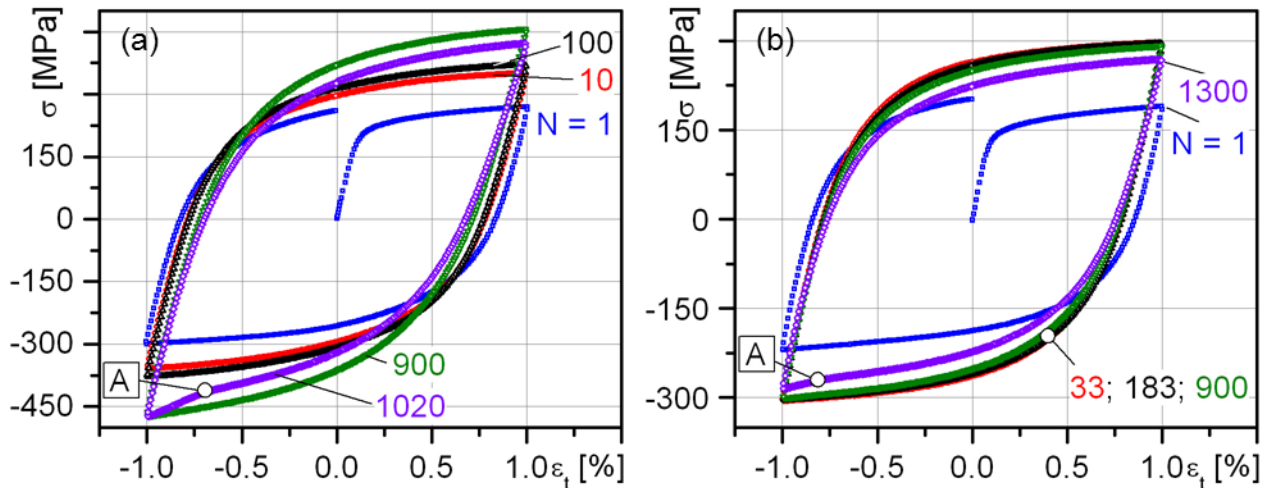


Figure 7. Stress-strain-hysteresis at ambient temperature (a) and $T = 300\text{ °C}$ (b)

The time of flight-total-strain-relationship (tof- ε_t) provides, in analogy to the stress-strain hysteresis, information about the actual state of fatigue of the austenitic steel. In the range of elastic-plastic material behavior, the tof- ε_t relation leads to a hysteresis-relationship (Figure 8a) for fatigue tests at ambient temperature and 300 °C (Figure 8b). It can be seen, that an increase/decrease of total-strain (ε_t) leads to increase/decrease of the tof signal. Due to elastic-plastic material behavior, microstructural changes like e. g. increase of dislocation density lead to an increase of the mean value of tof and shift the hysteresis-loop to higher values with increasing number of cycles. In tests at ambient temperature further cycling leads to deformation-induced α' -martensite (Figure 4a), which correlates with an increase of the mean value of tof. Due to changes in dislocation arrangement in tests at 300 °C cyclic softening occurs after $N = 183$ cycles, which leads to a decrease of the mean value of tof. Furthermore the tof- ε_t -relationship depends on micro and macro-crack initiation and propagation, which also shifts the hysteresis-loop to higher values along the ordinate. In comparison to the σ - ε -hysteresis (Figure 7), a significant change in the shape of the tof- ε_t -hysteresis loop occurs.

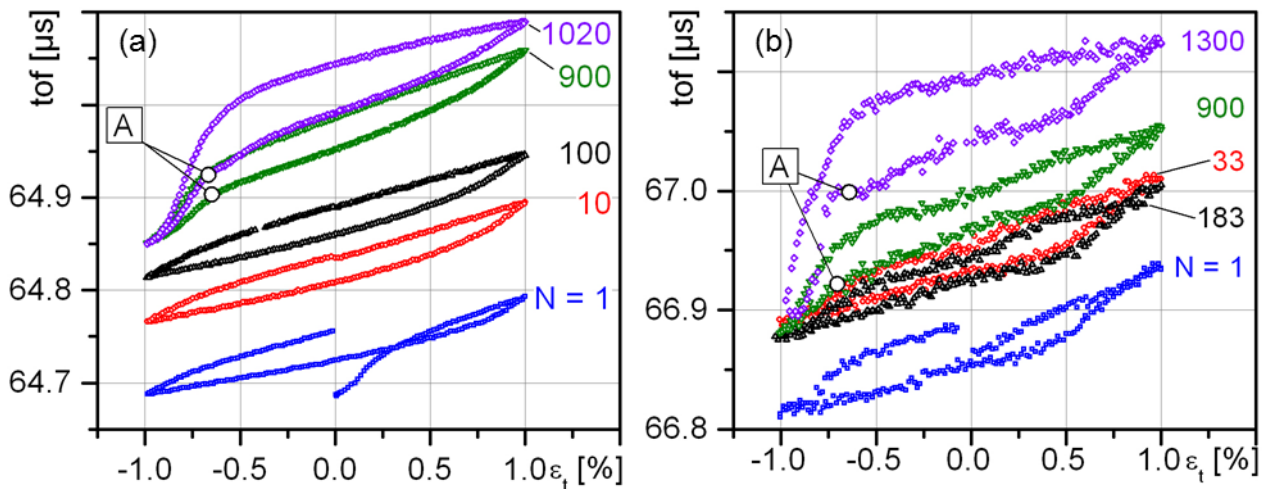


Figure 8. Correlation between time of flight (tof) and total-strain (ϵ_t) at ambient temperature (a) and $T = 300\text{ }^\circ\text{C}$ (b)

In analogy to σ - ϵ_t - and tof - ϵ_t -hysteresis, the relationship between the electromagnetically activated ultrasonic amplitude (peak) and total-strain (ϵ_t) was investigated in fatigue tests at ambient temperature (Figure 9a) and $300\text{ }^\circ\text{C}$ (Figure 9b). Generally an increase/decrease of ϵ_t leads to decrease/increase of peak. The peak is a physically based data, which in comparison to the above mentioned values, describes most sensible the occurrences of macro-crack and less sensible the change in dislocation density and arrangement or initiation of micro-cracks. Hence critical values of the change in the electromagnetically activated ultrasonic amplitude can be defined for structural health monitoring applications, which correlate with macro-cracks.

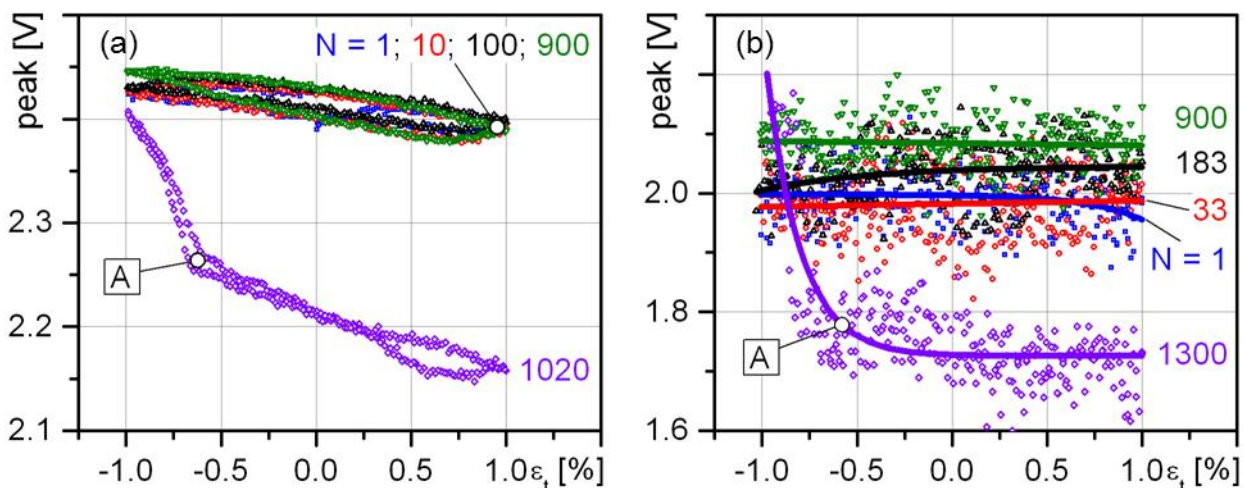


Figure 9. Correlation between electromagnetically activated ultrasonic amplitude (peak) and total strain (ϵ_t) at ambient temperature (a) and $T = 300\text{ }^\circ\text{C}$ (b)

3. Conclusions

In total strain controlled fatigue tests at ambient temperature and $T = 300\text{ }^\circ\text{C}$ the fatigue behavior of the austenitic steel AISI 347 was investigated by conventional stress-strain-hysteresis (σ - ϵ) measurements and by continuous, in-situ ultrasonic measurements generated with electromagnetic acoustic transducers (EMATs). Far reaching cross effects of EMAT and mechanical strain

measurements enable the recording of a hysteresis relation between time of flight (tof) and total-strain (ϵ_t) as well as relationship between the electromagnetically activated ultrasonic amplitude (peak) and total-strain (ϵ_t). The tof- ϵ_t -hysteresis gives, in analogy to the stress-strain-hysteresis, information about the cyclic hardening and/or softening processes, micro- and macro-crack initiation and propagation. Due to the occurrence of micro-cracks a significant change in the shape of the tof- ϵ_t -hysteresis curve can be detected earlier compared to σ - ϵ -hysteresis measurements. The significant changes in the peak values correlate with the development of macro-cracks. This effect can be used for the early detection of critical fatigue states before final failure in the sense of structural health monitoring.

Acknowledgements

This research work was carried out within the framework of the R&D in the Nuclear Safety Research Program, financed by Federal Ministry of Economy and Technology (BMWi), project number: 1501379, Germany. We also thank the German Research Foundation for financial support of the work. The used EMAT probes were developed at the Fraunhofer Institute for Non-Destructive Testing (IZFP), Saarbrücken, Germany. We thank the director of the IZFP, Prof. C. Boller and his coworkers, R. Tschuncky, I. Altpeter and G. Dobmann for their very helpful support.

References

- [1] J. Rudolph, S. Bergholz, A. Willuweit, M. Vormwald, K. Bauerbach, Methods of detailed thermal fatigue evaluation of nuclear power plant components, *Mat.-wiss. u. Werkstofftech.* 42, (2011) 1082-1092.
- [2] K.H. Lo, C.H. Shek, J.K.L. Lai, Recent developments in stainless steels, *Mater. Sci. Eng. R-Rep R65* (2009) 39-104.
- [3] M. Bayerlein, H.J. Christ, H. Mughrabi, Plasticity-induced martensitic-transformation during cyclic deformation of AISI 304L stainless-steel, *Mat. Sci. Eng. A* 114, (1989) L11-16.
- [4] M. Smaga, F. Walther, D. Eifler, Deformation-induced martensitic transformation in metastable austenitic steels, *Mat. Sci. Eng. A* 483-484, (2008) 394-397.
- [5] M. Smaga, F. Hahnenberger, A. Sorich, D. Eifler, Cyclic deformation behavior of austenitic steels in the temperature range $-60\text{ °C} \leq T \leq 550\text{ °C}$, *KEM* 465, (2011) 439-442.
- [6] V.S. Srinivasan, M. Valsan, R. Sandhya et al., High Temperature Time-Dependent Low Cycle Fatigue Behaviour of a Type 316L(N) Stainless Steel, *International Journal of Fatigue* 21, (1999) 11-21.
- [7] H. Mughrabi, H.J. Christ, Cyclic Deformation and Fatigue of Selected Ferritic and Austenitic Steels: Specific Aspects, *ISIJ International* 37, (1997) 1154-1169.
- [8] I. Altpeter, G. Dobmann, C. Boller et al. and M. Smaga, A. Sorich, D. Eifler, Early detection of damage in thermo-cyclically loaded austenitic materials, *Electromagnetic Nondestructive Evaluation XV*, IOS Press, 36, (2012) 130-139.
- [9] H.J. Salzburger, EMAT's and its Potential for Modern NDE - State of the Art and Latest Applications, *IEEE International Ultrasonics Symposium 1* (2009), 621-628.